Structural Features of Cross-Bridges in Isometrically Contracting Skeletal Muscle

Theresia Kraft,* Thomas Mattei,* Ante Radocaj,* Birgit Piep,* Christoph Nocula,* Markus Furch,† and Bernhard Brenner*

*Molecular and Cellular Physiology, Medical School, D-30625 Hannover, Germany; and †MPI for Medical Research, D-69120 Heidelberg, Germany

ABSTRACT Two-dimensional x-ray diffraction was used to investigate structural features of cross-bridges that generate force in isometrically contracting skeletal muscle. Diffraction patterns were recorded from arrays of single, chemically skinned rabbit psoas muscle fibers during isometric force generation, under relaxation, and in rigor. In isometric contraction, a rather prominent intensification of the actin layer lines at 5.9 and 5.1 nm and of the first actin layer line at 37 nm was found compared with those under relaxing conditions. Surprisingly, during isometric contraction, the intensity profile of the 5.9-nm actin layer line was shifted toward the meridian, but the resulting intensity profile was different from that observed in rigor. We particularly addressed the question whether the differences seen between rigor and active contraction might be due to a rigor-like configuration of both myosin heads in the absence of nucleotide (rigor), whereas during active contraction only one head of each myosin molecule is in a rigor-like configuration and the second head is weakly bound. To investigate this question, we created different mixtures of weak binding myosin heads and rigor-like actomyosin complexes by titrating MgATPγS at saturating [Ca^{2+}] into arrays of single muscle fibers. The resulting diffraction patterns were different in several respects from patterns recorded under isometric contraction, particularly in the intensity distribution along the 5.9-nm actin layer line. This result indicates that cross-bridges present during isometric force generation are not simply a mixture of weakly bound and single-headed rigor-like complexes but are rather distinctly different from the rigor-like cross-bridge. Experiments with myosin-S1 and truncated S1 (motor domain) support the idea that for a force generating cross-bridge, disorder due to elastic distortion might involve a larger part of the myosin head than for a nucleotide free, rigor cross-bridge.

INTRODUCTION

Conformational changes of the actin-attached myosin heads (cross-bridges) are generally thought to be responsible for force generation in skeletal muscle. However, the precise features of these structural changes remain unclear. In most of the recent concepts about the nature of the structural changes underlying force generation it is assumed that active force results from a conformational change of the actin-attached cross-bridge toward the rigor complex, i.e., it is assumed that the rigor-like cross-bridge represents the force generating structure of the myosin head. Particularly, models derived from protein crystallography of the isolated myosin head are based on this idea (Rayment et al., 1993; Holmes, 1997; Geeves and Holmes, 1999).

Development of force, however, is coupled to an elastic deformation of the myosin head while it is bound to actin with high affinity. Therefore, the structural features of the force generating cross-bridges states particularly under isometric conditions, i.e., when filament sliding is prevented, can only be studied in the three-dimensional lattice of muscle fibers. Previous x-ray diffraction (Huxley and Brown, 1967; Haselgrove, 1975; Huxley et al., 1982; Rapp et al., 1991), electron microscopy (Hirose et al., 1993), and electron paramagnetic resonance spectroscopy (Cooke et al., 1982, 1984; Roopnarine and Thomas, 1995) failed to provide evidence for a rigor-like complex formed during isometric contraction (e.g., no significant labeling of the actin layer lines in x-ray diffraction patterns). Alternatively, based on several lines of evidence, it was suggested that during isometric contraction, force-generating cross-bridges are in a conformation, which is different from the rigor complex. Some electron paramagnetic resonance spectroscopy suggested that a large disordered nonrigor-like population of cross-bridges contributes to force generation (Fajer et al., 1990). The different shape of diffuse x-ray scattering in frog muscle during isometric contraction versus rigor also was interpreted to indicate a "preferred" but not rigor-like configuration of the cross-bridges (Poulsen and Lowy, 1983; Lowy and Poulsen, 1987). Equatorial intensities and resistance to osmotic compression also revealed distinctly different geometries for actomyosin complexes during force generation versus cross-bridges in rigor (Brenner and Yu, 1993; Brenner et al., 1996).

However, it could be argued that all these apparent differences between cross-bridges attached in rigor and during force generation simply arise from the possibility that in rigor both heads of a myosin molecule simultaneously form a rigor complex, whereas during active force generation only one of the two heads forms the rigor complex and the second head is in a weak binding conformation. Thus, it may be concluded that the difference between a force generating and a rigor cross-bridge results from 1) different

Submitted May 2, 2001, and accepted for publication January 31, 2002.

Address reprint requests to Theresia Kraft, Molecular and Cellular Physiology Medical School, D-30625 Hannover, Germany. Tel.: 49-511-532-2734; Fax: 49-511-532-4296; E-mail: kraft.theresia@mh-hannover.de.

0006-3495/02/05/2536/12 $2.00

strain experienced in "double-headed" versus "single-headed" rigor complexes and 2) from different labeling patterns when in active contraction overall fewer heads are attached to actin filaments in a rigor-like configuration. To resolve these opposing views we developed an experimental approach in which the number of rigor complexes going from double-headed to single-headed rigor-like attachment could be varied by titrating the nucleotide analog MgATPγS.

In the present study, two-dimensional x-ray diffraction patterns of rabbit psoas muscle were recorded during rest, active contraction, and rigor. These patterns were compared with patterns recorded at different concentrations of MgATPγS and saturating [Ca^{2+}]. This allowed us to answer the question whether the active pattern, and in particular the 5.9-nm actin layer line, arises from a mixture of weakly bound and single-headed rigor-like cross-bridge states attached to actin. We used chemically skinned single fibers, a preparation that has several essential advantages over the widely used intact frog muscle. 1) It can be put into rigor within seconds without detectable loss of structural order (Brenner et al., 1984), which is essential for a quantitative comparison of the diffraction patterns. 2) It enables recording of two-dimensional x-ray diffraction patterns in the presence of nucleotide analogs or with exogenous myosin subfragment-1 (S1). 3) As shown previously (Kraft et al., 1999) with single fibers, diffusion and equilibration of substrates and products are much faster than in whole muscle preparations or muscle fiber bundles. This is particularly important because nucleotide depletion and accumulation of hydrolysis products, such as inorganic phosphate, must be avoided. For example, during isometric contraction, nucleotide depletion in the core of the preparation could mimic rigor-like features in the diffraction pattern. To obtain sufficient intensity from single fibers even for analysis of the much weaker off-meridional layer lines, arrays of single fibers were generated by mounting some 30 single fibers side by side into the x-ray beam. Earlier control experiments showed that even when single fibers are grouped together in small arrays, the gaps between individual fibers ensure that diffusion and equilibration take place like in single fibers (Kraft et al., 1999). This is different from natural muscle fiber bundles in which the gaps between individual fibers are very narrow.

The patterns obtained during isometric contraction showed a prominent intensity increase of the 5.9- and 5.1-nm actin layer lines and a significant enhancement of the first actin layer line (at 37 nm) compared with relaxing conditions. Quite surprisingly, however, we observed distinctly different intensity distributions along the 5.9-nm actin layer line under isometric conditions compared with rigor and relaxation. Furthermore, the diffraction pattern and particularly the 5.9-nm actin layer line profile recorded in isometric contraction could not be matched by mixtures of weak binding cross-bridges and rigor-like complexes, simulated by different ATPγS-concentrations, i.e., even under conditions where one-headed rigor-like binding of the cross-bridges to actin occurred. A preliminary account of this work was presented earlier (Kraft and Brenner, 1997a).

MATERIALS AND METHODS

Fiber preparation

Small bundles of skeletal muscle fibers from rabbit psoas muscle were excised and chemically skinned with 0.5% Triton-X-100 as described earlier (Brenner, 1983; Yu and Brenner, 1989; Kraft et al., 1995). Immediately after the skinning procedure, single fibers were isolated and kept (for up to 2 days) in skinning solution without Triton until they were mounted for the experiment. Storage of single fibers instead of bundles resulted in a very good preservation of the regulatory properties and an optimal structural stability of the fibers.

NEM-S1 and truncated S1

N-ethyl-maleimide (NEM)-modified S1 was obtained by *N*-ethyl-maleimide-modification of S1 that was enzymatically isolated from rabbit back muscle (modified after Williams et al., 1984). Truncated S1 (motor domains) of *Dictyostelium* myosin were generated using a *Dictyostelium* expression system (Furch et al., 1998). The S1 was truncated at position 765, and 20 extra amino acids were added to the actin-binding surface loop (loop 2). These extra amino acids replace the segment of loop 2 between residues 618 and 622 and add 12 positive charges to this loop. The additional charges result in an increase in actin affinity of the motor domain such that its affinity is close to that of rabbit S1.

Solutions

All chemicals except where noted were from Sigma (St. Louis, MO). Skinning solution, relaxing solution, preactivating, and activating solution were composed as described previously (Kraft et al., 1995, 1999). To ensure sufficient nucleotide supply during the entire period of isometric contraction (200–300 s), preactivating and activating solutions contained 2 mM MgATP and an ATP-backup system of 10 mM creatine phosphate and 500 Units/mL creatine phosphokinase. MgATPγS-solutions were prepared after purification of ATPγS (Boehringer Mannheim, Indianapolis, IN) as previously described (Kraft et al., 1992), except for the addition of 0.01 U/mL apyrase at 1 mM MgATPγS. For lower MgATPγS concentrations, hexokinase and apyrase concentrations were reduced in proportion to the MgATPγS concentration.

To immediately remove the MgATP when transferring the fibers from relaxing solution into rigor, the single fiber preparation was incubated in a "quick rinse" solution for several minutes. Quick rinse solution contained 10 mM imidazole, 2.5 mM EGTA, 7.5 mM EDTA, and 135 mM potassium propionate. For recording of the x-ray diffraction patterns fibers were then transferred directly into rigor solution containing 10 mM imidazole, 2.5 mM EGTA, 2.5 mM EDTA, 140 mM potassium, 5 mM dithiothreitol, 10 mM glutathione, and 1000 U/mL catalase. The pH of all solutions was set to 7.0 at the respective experimental temperature, and ionic strength was adjusted with potassium propionate.

For minimizing beam damage, all solutions used for x-ray diffraction experiments contained 5 mM dithiothreitol, 1000 U/mL catalase, and 10 mM glutathione, and the maximal acceptable exposure time was limited to a few hundred seconds, determined as in Kraft et al. (1999). The fibers were scanned vertically in the x-ray beam so that 6 mm of the muscle length were irradiated. The scanning speed was 1 to 2 mm/s. Furthermore, in each experiment the diffraction patterns under the different conditions were recorded in random order to avoid artifacts due to possible beam damage.

Mounting of the single fibers

The specimens for recording of the diffraction patterns were prepared according to the method described in detail in Kraft et al. (1999). To avoid problems with diffusion and equilibration of substrates and products throughout the specimen, we used single fibers instead of natural fiber bundles for all experiments shown here. To obtain sufficient intensity not only in equatorial and meridional reflections but also in the off-meridional layer lines of the diffraction patterns, for each experiment ~30 single fibers were mounted side by side into the x-ray setup. Previously we showed that diffusion of substrates into single fibers mounted side by side into arrays is like diffusion into individual single fibers and thus quite different from diffusion into natural fiber bundles (Kraft et al., 1999). In natural bundles the fibers are densely packed without much space between them so that diffusion occurs only from the outer surface of the whole bundle. Depending on the diameter, in these bundles it takes much longer until the fibers in the center of the bundles are equilibrated. In contrast, in single fiber arrays, i.e., when fibers are first isolated as single fibers and subsequently mounted side by side into the experimental chamber, diffusion occurs from the relatively large gaps between the fibers into each individual fiber. This means that, independent of the size of the preparation, the fibers in the center of such arrays are equilibrated with the same time course as fibers in the outer parts, i.e., all fibers equilibrate like individual single fibers (compare Fig. 4 in Kraft et al., 1999). To further minimize concentration gradients (and also temperature gradients) within the preparation and particularly in the small gap between the kapton windows, the solution in the experimental chamber was permanently pumped up and down (flow rate ~1 mL/min).

Each array of single fibers was ~1-mm wide, 0.3-mm thick, and had a free length of ~22 mm. Fibers were mounted side by side, and care was taken to maintain the same sarcomere length for all fibers. Before the experiment sarcomere length was adjusted to 2.4 μm, using laser light diffraction as control. The ends of the isolated single fiber segments (length ~28 mm) were attached to stainless steel holders, which were first covered with 3145RTV silicone glue (Dow Corning, Midland, MI). Different from the previous work (Kraft et al., 1999), fibers were finally glued to the fiber holders with Histoacryl (Braun, Melsungen, Germany). The experimental chambers were modified so that the upper fiber holder was attached to a linear motor, which allowed rapid unloading of the fibers with subsequent restretch to the original length. The lower fiber holder was replaced by a force transducer (SensoNor, Horten, Norway). The temperature-controlled muscle chambers with the single fiber arrays were mounted vertically for the x-ray exposures.

Experimental protocols

During isometric contraction fibers were stabilized by applying a quick-release protocol (Brenner, 1983). For recording of x-ray diffraction patterns during isometric contraction, data were accumulated in the isometric periods of the quick-release protocol only. The stability of the striation pattern was monitored by projecting the laser diffraction pattern onto a screen. NEM-S1 and S1 motor domain fragments were diffused into single fiber arrays either at normal sarcomere length (2.4–2.5 μm) or after pulling the fibers slowly to very long sarcomere length (~4.0 μm). To study effects of binding of NEM-S1 or of the S1 motor domain to actin, two-dimensional x-ray diffraction patterns were recorded before and after 6 to 24 h of incubation with the respective protein under rigor conditions. Full saturation of all binding sites along the thin filaments with the externally added myosin fragments was not anticipated.

X-ray diffraction and data reduction

Two-dimensional x-ray diffraction patterns were recorded at station 2.1 of the SRS in Daresbury, Great Britain, using a position sensitive two-dimensional multiwire detector. All patterns were recorded from single fiber arrays, a method developed at the EMBL-beamline X-13 of the Deutsches Elektronen Synchrotron (DESY) in Hamburg, Germany (Kraft et al., 1999). The specimen-to-detector distance was 2.85 m.

The data were analyzed on an Silicon Graphics INDIGO workstation with the programs "bsl" and XOTOKO of the CCP13 software package provided by the SRS Daresbury. For data analysis the diffraction patterns were corrected for uneven detector response and normalized to the ionization chamber, i.e., to the intensity of the incoming beam. At the end of each experiment background patterns were recorded with exactly the same camera configuration and exactly the same position and geometry of the muscle chamber. To achieve this, all muscle fibers were removed through prolonged activation and stretching of the fibers until they were ripped apart, followed by overcontraction. The camera background was subtracted from each pattern so that the intensity of the attenuated main beam, which had passed through a semitransparent beam stop, was practically zero. Subtraction of the camera background allowed us to normalize the overall intensities of all patterns to the overall intensity of the patterns in rigor since for the limited detecting area total integrated intensity scattered by a muscle sample is the same for all conditions. For comparing absolute intensities, this normalization was necessary to account for possible movement of the muscle fibers in the beam or sporadic loss of a fiber during contraction, two factors that could have changed the amount of diffracting mass in the x-ray beam.

The diffraction patterns were rotated and shifted so that patterns that were recorded under identical conditions could be added together. The added patterns were folded, and profiles in horizontal and vertical direction were obtained for further analysis. The profiles of all actin layer lines shown here (Figs. 1, 2, and 4) were obtained by integrating the intensity of the respective layer line in a series of 19 to 22 vertical sections parallel to the meridian. This series of vertical sections covers the area from the center of the meridian to the edge of the pattern at a radial spacing of approximately 0.25 nm^{-1} (Figs. 1, 3, and 5). A gauss-function was fitted to the respective peaks of a series of sections after the background under the peaks had been subtracted using the software ORIGIN (Microcal, Northampton, MA). The peak intensities of the individual sections were plotted as a function of the radial position of the respective section. Noise in the 5.1-nm actin layer line profiles in Fig. 2 *A* as well as in the difference traces in Figs. 4 and 5 was reduced by a five-point adjacent averaging routine (ORIGIN, Microcal). Lattice spacings were calibrated as described earlier (Xu et al., 1997; Kraft et al., 1999).

RESULTS

Isometric contraction, relaxation, and rigor

To characterize the structural features of strongly bound cross-bridges in isometrically contracting arrays of single muscle fibers we recorded two-dimensional x-ray diffraction patterns during isometric steady-state contraction, under relaxing conditions, and in rigor. The experiments were carried out at 80 mM ionic strength to obtain a rather large fraction of cross-bridges attached to actin in relaxation and isometric contraction. The low temperature was chosen to increase the structural stability of the muscle fibers during isometric contraction. Isometric force generation under these conditions, measured in separate mechanical experiments together with fiber ATPase activity and other parameters, was found to be 78 ± 11 kN/m^2 (n = 5 fibers). This

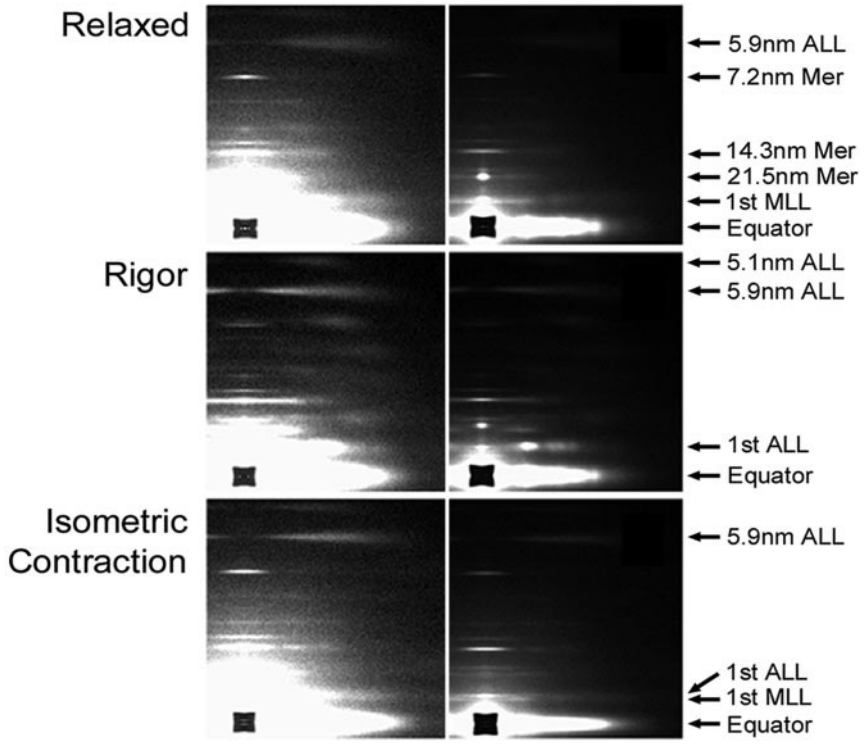

FIGURE 1 Two-dimensional x-ray diffraction patterns recorded from six single fiber arrays under relaxation, in rigor, and during isometric contraction (pCa 4.5). All conditions were recorded with each array of single fibers. Total added exposure time of all six single fiber arrays was 1200 s for each condition (~200 s for each single fiber array). Patterns were folded, i.e., all four quadrants were averaged. (*Right one-half of the figure*) Lower display intensity to show stronger reflections; (*left one-half*) higher display intensity for weaker reflections. T = 1°C, ionic strength = 80 mM. Note that during isometric contraction the first actin layer line (ALL) at 37 nm and the first myosin layer line (MLL) at 43 nm are well resolved (compare lower panel, right hand side). Mer, Meridional reflection; 14.3-nm Mer corresponds to the so-called M3 reflection.

is approximately one-half of the maximal active force observed in frog fibers under physiological conditions. Isometric force of the psoas muscle fibers increased to ~170 kN/m^2 when temperature was raised to 20°C.

In agreement with previous studies (e.g., Haselgrove, 1975; Huxley et al., 1982), Fig. 1 shows that during isometric contraction at 1°C and 80 mM ionic strength, the 21.5-nm meridional reflection essentially disappears, whereas the intensities of the 14.3- and 7.2-nm meridional reflections increase compared with relaxing conditions and rigor. Because with the single fiber array the actin and myosin components of the first layer line complex are well resolved (e.g., first actin layer line at 37 nm versus first myosin layer line at 43 nm in Fig. 1) both layer lines were fitted separately for analysis. Intensity profiles (Fig. 2) indicate that the intensities of the first, the 5.9-nm and the 5.1-nm actin layer lines increase quite substantially when going from relaxation to isometric contraction and even more when going into rigor. Different from most previous studies, it was found that when changing from relaxation to isometric contraction the intensity distribution along the 5.9-nm actin layer line is clearly shifted toward the meridian (to smaller reciprocal spacing in Fig. 2 *B*). In rigor the intensity maximum is even closer to the meridian. Note that on the first actin layer line lattice sampling in rigor (spots of high intensity in Fig. 1, right one-half of the middle panel) causes an intensity modulation resulting in peaks of very high intensity at the radial spacing of the equatorial reflections. Because such sampling is not present during isometric contraction, this layer line cannot be used for a quantitative comparison of the changes in the intensities and intensity distribution along this layer line. The 5.9- and 5.1-nm actin layer lines, however, are not affected by lattice sampling (see also Huxley and Brown, 1967). We therefore had to restrict the quantitative analysis to these two actin-based layer lines. The relative intensity increases of the 5.1- and 5.9-nm actin layer lines are shown in Table 1.

MgATPγS-titration

To examine whether the diffraction pattern under isometric conditions, specifically the intensity distribution along the 5.9- and 5.1-nm actin layer lines could result from a mixture of weakly bound and single-headed rigor-like actomyosin complexes, different mixtures of weak binding and nucleotide-free, rigor-like cross-bridges were generated by incubating fibers in different concentrations of MgATPγS (Kraft et al., 1992, 1998, 1999). To ensure conditions comparable with isometric contraction, titration was carried out at saturating [Ca^{2+}] (pCa 4.5). It has been shown earlier (Kraft et al., 1992) that increasing the MgATPγS concentration from nucleotide-free to saturating MgATPγS concentration at high [Ca^{2+}] results in a rather wide and shallow titration curve, allowing measurements over a wide range of nucleotide concentrations. In the course of such a titration, starting from rigor, it is expected that nucleotide-free myosin heads with highest strain will be the first to bind

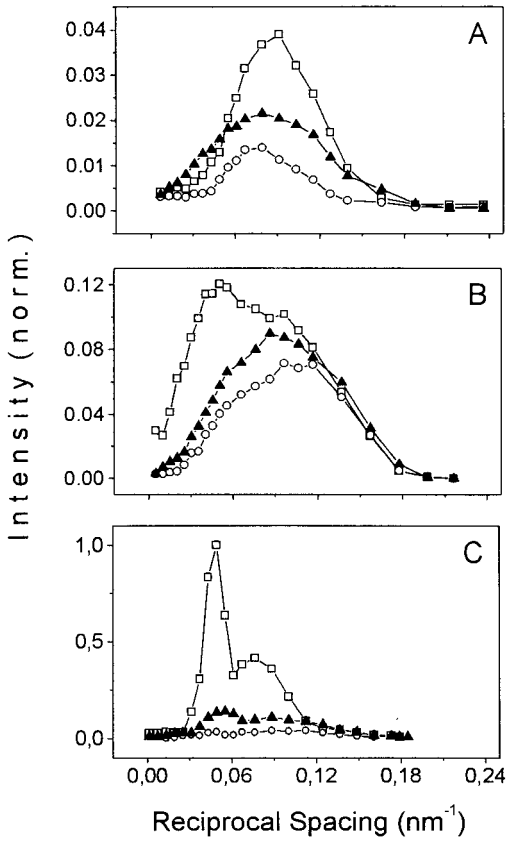

FIGURE 2 Intensity profiles from the diffraction patterns shown in Fig. 4 of the actin layer line at 5.1 nm (*A*), at 5.9 nm (*B*) and of the first actin layer line (*C*). All intensities normalized to maximal intensity of first actin layer line in rigor. Rigor (□); isometric contraction (▲); relaxing conditions (○). (*C*, ○) The reduction in intensity upon raising [Ca^{2+}] to saturating levels was taken into account (Yagi and Matsubara, 1988; MgATPγS ± calcium at long sarcomere length; own unpublished results). The first actin layer line profile was obtained by fitting also the neighboring first myosin layer line and the meridional troponin reflection.

nucleotide and detach (Hill, 1974). Thus, at low MgATPγS concentration one head of double headed rigor-complexes is expected to bind nucleotide and detach, thereby releasing the strain generated by the double-headed binding. As a consequence, the remaining nucleotide-free rigor-like head binds the nucleotide less tightly, i.e., only at higher nucleotide concentrations. Therefore, the titration allows us to investigate possible effects of single-headed versus double-headed rigor-like attachment on the actin layer line profiles.

Examples of diffraction patterns at different MgATPγS-concentrations are shown in Fig. 3. None of the diffraction patterns recorded in the presence of MgATPγS matched the patterns recorded under isometric contraction. To better illustrate the changes of the layer line profiles, in Fig. 4 the difference traces of the various profiles of the 5.9-nm actin layer line are shown. For these difference traces the profile recorded under relaxing conditions was subtracted from the profiles recorded in isometric contraction, rigor, and at 20 μM, 100 μM, and 1 mM MgATPγS. Thus, each difference trace represents the profile of the increase in intensity when going from relaxing conditions to active, rigor, or different MgATPγS-concentrations, respectively. Fig. 4 *A* shows that at any MgATPγS-concentration, i.e., with any mixture of nucleotide-free, single-headed, rigor-like cross-bridges and weak binding cross-bridges, the intensification of the 5.9-nm actin layer line always has its maximum at the same position as in rigor near the meridian. There is no indication of a shift of this profile due to the release of rigor cross-bridges with highest strain at the lowest MgATPγS concentration. Yet, for isometric contraction the maximum of the intensification of the 5.9-nm layer line relative to relaxing conditions is substantially further away from the meridian (Fig. 4 *B*). This demonstrates that it is not possible to mimic the 5.9-nm actin layer line profile observed under isometric contraction by a mixture of weak-binding and rigor-like cross-bridges.

TABLE 1 Intensification of the 5.9- and 5.1-nm actin layer lines and calculated fractions of strongly attached cross-bridges ("set 2" corresponds to Fig. 1)

	$\Delta I_{Isometric}/\Delta I_{Rigor}$*	Fraction (*n*) from square law	Fraction (*n*) from modeling
5.1 nm (set 2†)	0.58	0.76	0.75
5.9 nm (set 2†)	0.33	0.57	0.45
5.9 nm (set 1†)	0.41	0.64	0.54

*The intensity of each layer line profile was integrated. From the intensity in contraction and rigor the intensity under relaxing conditions was subtracted. A 7% increase of 5.9-nm actin layer line and a 4.5% increase of 5.1-nm actin layer line due to calcium activation of the thin filament (and not from cross-bridge attachement) was taken into account. The intensity increase under isometric contraction was determined relative to the increase in rigor (e.g., $I_{Isometric} - I_{(Rel.+7\%)}/I_{Rigor} - I_{(Rel.+7\%)}$).

†("Set 1" and "set 2," respectively, are two different data sets that were obtained during separate sessions at the synchrotron. In our first set of diffraction patterns the 5.1-nm actin layer line was cut off partially so that it could not be included in the analysis.

Actin labeling by binding of myosin subfragment-1 (NEM-S1) versus truncated S1

The MgATPγS experiments suggest that the difference between the diffraction patterns and particularly the intensity distribution along the 5.9-nm actin layer line in rigor versus isometric contraction arises from a structural difference between actin-attached cross-bridges in rigor and cross-bridges that generate active force. For instance, the greater intensification closer to the meridian in rigor might result from the myosin heads being stereospecifically bound to actin and highly ordered, i.e., with little distortion up to a rather high radius from the axis of the actin filament. Under isometric conditions, only a smaller part of each stereospecifically bound myosin head might follow the geometry of the F-actin helix, whereas the parts of the head further away from the actin filament axis are disordered.

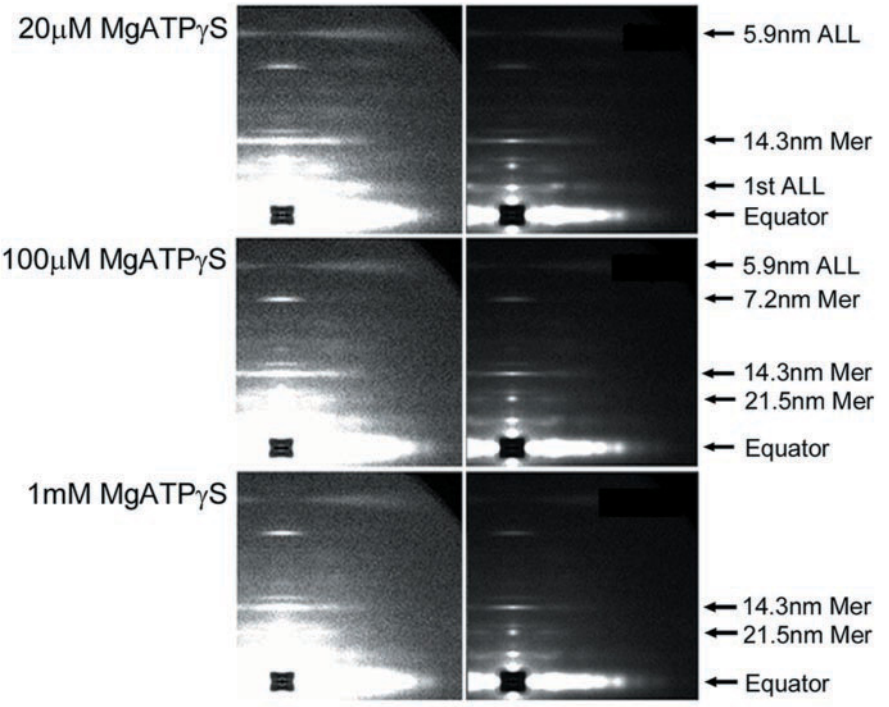

FIGURE 3 Two-dimensional x-ray diffraction patterns in the presence of three different concentrations of MgATPγS at saturating [Ca^{2+}] (pCa 4.5). Patterns for all these conditions were recorded from four single fiber arrays. The resulting total added exposure time was 150 s for each condition. The patterns were treated as described in Fig. 1. Note the difference of several features between these diffraction patterns and the one recorded in isometric contraction (Fig. 1, *lower panel*), e.g., the essential absence of the meridional reflection at 21.5 nm during isometric contraction and the difference in the intensity profile of the 14.3-nm meridional reflection.

This possibility was tested by diffusing myosin S1 or NEM-modified S1 (NEM-S1) as well as truncated S1 (motor domain only) into single fibers under rigor conditions. It was reasoned that the truncated S1 simulates the situation of an ordered motor domain with a highly disordered light chain-binding domain that does not contribute to the layer lines. Fig. 5 *A* shows parts of the patterns recorded with NEM-S1 and truncated S1 after subtracting the rigor patterns obtained before diffusion of the exogenous protein (difference patterns). Binding of NEM-S1 (or S1, data not shown) to actin causes an intensity increase of the 5.9-nm actin layer line with the maximum closer to the meridian than the intensity increase with truncated S1 (Fig. 5 *B*). In fact, the intensity increase upon binding of NEM-S1 (or S1) occurs at essentially the same radial spacing as the intensity increase observed in fibers without added NEM-S1 (or S1) when changing from relaxation to rigor (cf. Fig. 4). The layer line profile upon binding of NEM-S1 (or S1), however, is different from the profile observed when truncated S1 (motor domain) is bound to the thin filaments (Fig. 5 *B*). At long sarcomere length we found a similar difference in the intensification of the 5.9-nm actin layer line upon binding of NEM-S1 versus binding of truncated S1 (data not shown). Altogether, these experiments qualitatively support

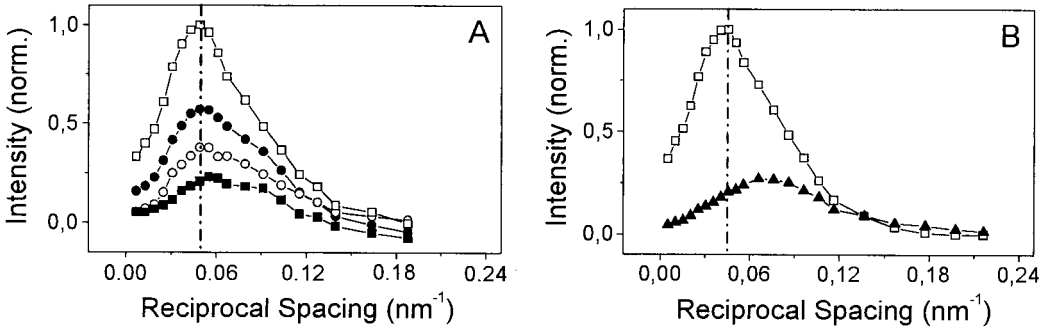

FIGURE 4 (*A*) Changes in intensity along the 5.9-nm actin layer line when going from relaxing conditions to different concentrations of MgATPγS at saturating [Ca^{2+}] (compare with Fig. 3) are compared with rigor conditions. The 5.9-nm actin layer line profile recorded under relaxing conditions was subtracted from all other 5.9-nm layer line profiles (difference traces). Rigor (□), 20 μM MgATPγS (●), 100 μM MgATPγS (○), 1 mM MgATPγS (■). (*B*) Change in intensity along the 5.9-nm actin layer line (compare with Fig. 2 *B*) when changing from relaxing conditions to rigor or isometric contraction. Again, the intensity profile recorded under relaxing conditions was subtracted from the profiles in rigor and active contraction. Rigor (□), isometric contraction (▲), respectively. $T = 1°C$, ionic strength = 80 mM. Intensity increases normalized to the maximal increase seen in rigor.

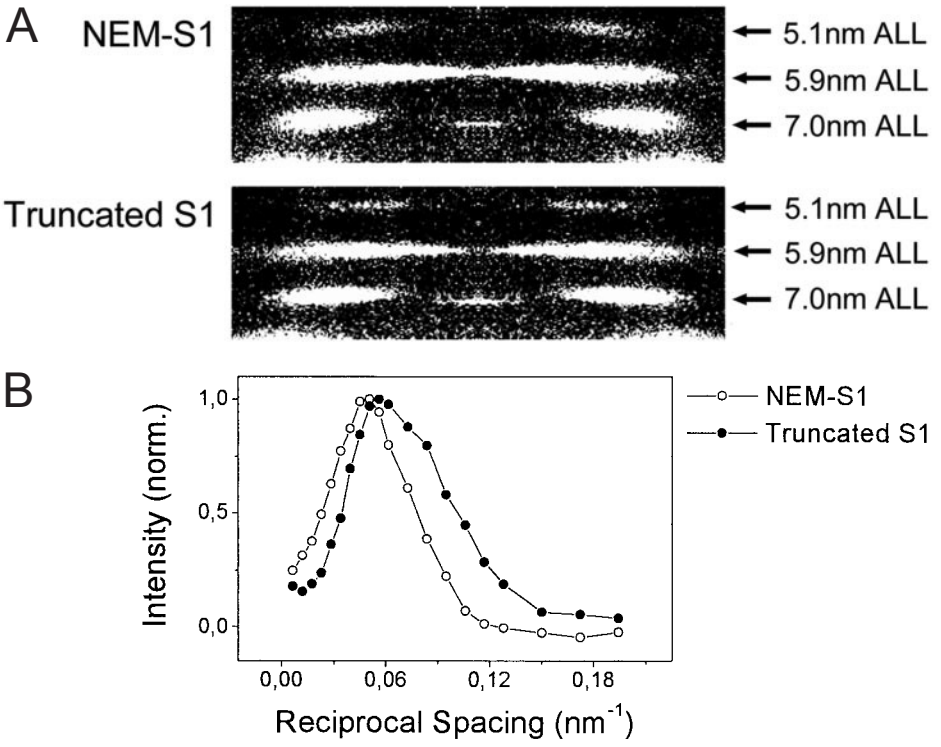

FIGURE 5 Intensification of actin based layer lines upon binding of NEM-S1 or truncated S1 to actin filaments under rigor conditions. (*A*) Parts of the difference patterns when either NEM-S1 (*upper panel*) or truncated S1 (motor domain; *lower panel*) is bound to actin under rigor conditions, $T = 1°C$, ionic strength = 80 mM. Only the 7.0-, the 5.9-, and 5.1-nm actin layer lines are shown. (*B*) Intensity increase along the 5.9-nm actin layer line due to binding of NEM-S1 (○) or truncated S1 (●), respectively. Intensities normalized to the maximal intensity increase. Difference patterns (*A*) and difference traces (*B*) were obtained by subtracting the rigor patterns/profiles recorded before exposure to the exogenous protein from the patterns/profiles recorded after equilibration with the exogenous protein.

the conclusion that the differences in 5.9-nm actin layer line intensity distribution between rigor and isometric contraction might be interpreted as the result of a structural difference between cross-bridges attached to actin in rigor and during force-generation. Specifically, the data shown in Fig. 5 are consistent with the idea that under isometric conditions a larger part of the attached cross-bridge is disordered.

DISCUSSION

Major findings of the present paper are an intensification of the first, the 5.9-nm, and the 5.1-nm actin layer lines and a remarkable shift in intensity distribution of the 5.9-nm actin layer line toward the meridian when changing from relaxation to isometric contraction. This shift in intensity distribution is different from the shift observed in rigor and could not be mimicked by mixtures of weakly bound cross-bridges and rigor-like actomyosin complexes, which were generated in the presence of different concentrations of MgATPγS at saturating [Ca^{2+}]. The profiles of the intensity changes on the 5.9-nm actin layer line at various MgATPγS-concentrations show that whenever there are some nucleotide-free rigor-like complexes in the fiber, the maximal contribution to the 5.9-nm actin layer line intensity remains essentially at the same position as found in rigor (Fig. 4). This position is also unaffected when, as expected from thermodynamics (Hill, 1974), at low nucleotide concentrations first one of the double-headed nucleotide-free actomyosin cross-bridges binds MgATPγS and dissociates. It thus releases some of the strain of the second nucleotide free head, resulting in a less strained, single-headed nucleotide-free cross-bridge. The titration with MgATPγS also enabled the possibility to be tested that the differences seen between rigor conditions and active contraction result from preferred binding of myosin heads to "target areas" (Squire, 1981), i.e., from systematic differences in accessibility of binding sites on actin filaments due to the mismatch between periodicities of the thin and thick filaments. It was hypothesized that in rigor the binding of all myosin heads to such target areas will result in larger average distortions than for active contraction if only at most one head per myosin molecule had to bind in a stereospecific rigor-like complex. If the shift of the intensity distribution along the 5.9-nm actin layer line between rigor and isometric contraction were due to different strain resulting from binding of myosin heads to target areas on actin, then a similar shift had been expected in the MgATPγS titration, where the number of nucleotide free rigor-like heads was systematically decreased. Taken together these results support the view, that cross-bridges being stereospecifically attached to actin during isometric contraction are not structurally equivalent to either single-headed or double-headed rigor-like cross-bridges.

For these experiments, however, two conditions had to be fulfilled: 1) MgATP-depletion and accumulation of hydrolysis products, which might occur during isometric contraction in the core of the muscle preparation, had to be minimized. Otherwise rigor-like features could appear in the

diffraction patterns of isometric contraction. 2) Titration of MgATPγS had to create random mixtures of weakly bound and rigor-like cross-bridges. This means that nucleotide depletion in the core of the muscle preparation, presumably due to cleavage of MgATPγS, had to be avoided. Otherwise, the rigor-like features in the patterns and intensity profiles at nonsaturating MgATPγS-concentrations would be affected by a nucleotide-free core of the preparation and would not result solely from single-headed rigor-like cross-bridges throughout the preparation. In the experiments presented here both requirements were met by using loose arrays of single, isolated muscle fibers instead of natural fiber bundles. As shown previously, the advantage of mounting single fibers side by side into the setup is that diffusion and equilibration of substrates and products occurs as in individual single fibers, i.e., much faster than in bundles (Kraft et al., 1999). When characterizing the preparation of single fiber arrays in our previous work we could show the effect of impaired diffusion on nucleotide saturation in natural fiber bundles. In contrast, diffusion (measured as saturation with nucleotide) in arrays of single fibers was the same as in individual single fibers (see Fig. 3 in Kraft et al., 1999). Based on these earlier control experiments it is reasonable to assume that neither in the MgATPγS titration experiments nor in isometric contraction or relaxation, diffusion and equilibration of substrates and products was limited due to the size of the muscle preparation. It can be concluded that in isometric contraction, the shift of the intensity distribution of the 5.9-nm actin layer line toward the meridian is not due to a fraction of nucleotide-free cross-bridges in the core of the preparation. Such depletion in fact should generate a change in the intensity profile with the maximal intensity increase at the position of the maximum in rigor. In the MgATPγS titration experiment the distribution of cross-bridge states throughout the preparation, e.g., rigor and weakly bound cross-bridges is expected to be random, just like in an individual single fiber. Thus, the resulting diffraction patterns and layer line profiles should represent random mixtures of weakly bound and rigor-like actomyosin complexes.

The nature of the structural difference between cross-bridges in rigor and during force generation might be derived from the observation that binding of truncated S1 (motor domain) to actin causes an increase of the 5.9-nm actin layer line with the maximal intensity increase further away from the meridian than observed upon binding of full-length S1 (Fig. 5). These findings are consistent with the idea that in rigor a larger portion of the attached myosin head, including part of the light chain-binding region follows the actin-based helical order. During isometric contraction, in contrast, a smaller part of the attached myosin head might follow the F-actin helix, whereas the light chain binding domain, possibly even including parts of the motor domain might be disordered.

The data presented here are in agreement with earlier predictions for stereospecific cross-bridge attachment, i.e., attachment in an actin-based helical order, which was expected to cause an increase in average radius of the actin filament and therefore not only an increase in actin layer line intensities but also a shift of the intensity maximum of the 5.9-nm actin layer line closer to the meridian (Huxley and Brown, 1967; Parry and Squire, 1973; Yagi and Matsubara, 1988). Yet, previously only an insignificant change in intensity distribution was found in some studies on frog muscle between relaxation and tetanic contraction (Haselgrove, 1975; Wakabayashi et al., 1985; Yagi and Matsubara, 1988) and during contraction at low versus high temperature (Tsaturyan et al., 1999). Perhaps such a shift escaped detection in most studies because of the very close proximity of the 5.9-nm actin layer line and the seventh myosin layer line (Kress et al., 1986). Because the myosin based layer lines are rather strong in frog muscle even at low temperature and in rabbit they are much weaker (Xu et al., 1987, 1997; Kraft et al., 1999), reciprocal intensity changes on myosin layer lines and actin layer lines during contraction might obscure the expected shift of the 5.9-nm actin layer line in frog muscle. This is supported by experiments on frog muscle at different temperatures where the contribution from the seventh myosin layer line was removed (Maeda et al., 1988). At 4°C and also at 10°C the 5.9-nm actin layer line showed a slight shift of the peak intensity toward the meridian compared with relaxing conditions, whereas at 20°C essentially no intensity increase was detectable in the frog data. Another reason for the often missing shift of the 5.9-nm actin layer line might be that intact frog muscle, different from skinned fibers, contains soluble proteins and other molecules that decrease the contrast in electron densities, resulting in a lower signal to noise ratio in the diffraction patterns.

A further question is, whether the low temperature (1°C) and relatively low ionic strength (80 mM) used in the present study might affect the intensity distribution, particularly on the 5.9-nm actin layer line. One might, for example, expect that due to the low temperature cross-bridges are trapped in other cross-bridge states than those populated at high temperature. From our earlier work, however, it can be concluded that the data obtained in this study at low temperature are also representative for structural features of force generating cross-bridges at higher, near physiological temperature. We previously found that the two- to threefold increase in isometric force when raising the temperature from 1°C to 20°C is associated with only a small increase in the fraction of strongly attached cross-bridges (Kraft and Brenner, 1997b). The observed increase in force was found to be mainly due to a higher force generated by the individual cross-bridge in each of the force generating states and not due to a redistribution of cross-bridges among different force-generating states (Brenner, 1991; Kraft and Brenner, 1997b). This indicates that at low and at high

temperature the occupancy of cross-bridge states is rather similar. Support for this conclusion was obtained in preliminary experiments where we recorded two-dimensional x-ray diffraction patterns during isometric steady-state contraction, under relaxing conditions, and in rigor at 20°C (Kraft et al., 2000). Under all three conditions the intensity distribution of the 5.9-nm actin layer line was very similar to the profiles shown here at 1°C (data not shown). In isometric contraction at 20°C, the 5.9-nm actin layer line was shifted by approximately the same amount toward the meridian as at 1°C. As mentioned above, a slight shift of the 5.9-nm actin layer line was also observed in frog muscle at 1°C and at 10°C (Maeda et al., 1988). Therefore it appears rather unlikely that the shift in intensity distribution found here for isometric contraction compared with relaxation and rigor is due to the low experimental temperature.

Fraction of stereospecifically attached cross-bridges during isometric contraction

To address the question whether the intensification of the actin layer lines during isometric contraction is consistent with a large fraction of stereospecifically and presumably strongly attached cross-bridges, we estimated the fraction of attached cross-bridges from the integrated intensities of the profiles shown in Fig. 2. Only the actin layer lines at 5.9 and 5.1 nm were used for this analysis because there is essentially no lattice sampling on these two layer lines (Huxley and Brown, 1967). Due to the very strong sampling on the first actin layer line in rigor this layer line cannot be used for a quantitative analysis. A control experiment in which the strongly sampled first actin layer line profile in rigor (Fig. 2 *C*) was compared with a profile recorded in rigor from muscle fibers with more disordered myofilaments showed that the disorder reduces not only the sampling but also the total integrated intensity of the first actin layer line. Consequently, we cannot compare the intensity of the sampled first actin layer line in rigor with the intensity of the unsampled layer line in isometric contraction to determine the fraction of stereospecifically attached cross-bridges during contraction.

The calculations of the fraction of stereospecifically attached cross-bridges from the intensities of the actin layer lines at 5.9 and 5.1 nm are based on 1) the assumption that in rigor all myosin heads are attached to actin (Cooke and Franks, 1980; Lovell and Harrington, 1981) and 2) that weakly bound cross-bridges under relaxing conditions do not affect the intensity of 5.1- and 5.9-nm actin layer lines to a measurable extent (Xu et al., 1987, 1997; Kraft et al., 1999). However, the effect of calcium binding to the thin filament, which causes an increase of 5.9-nm actin layer line intensity by 7% (Kraft et al., 1999), and an increase of 5.1-nm actin layer line by ~4.5% (authors unpublished data) was taken into account (Table 1). Earlier studies with frog muscle at long sarcomere length (i.e., beyond overlap between actin and myosin filaments) showed a very similar effect of calcium activation on 5.9-nm actin layer line (Kress et al., 1986; Yagi and Matsubara, 1988), which was suggested to be the result of calcium-induced actin subdomain movement together with an azimuthal shift of tropomyosin (Al-Khayat et al., 1995).

If we follow the arguments of others (Bershitsky et al., 1997; Tsaturyan et al., 1999) and assume that the intensity is proportional to the square of the number of diffractors (Haselgrove, 1975), i.e., ignore differences in the structures of rigor versus force generating cross-bridges, the fraction of strongly attached heads would be proportional to the square root of the integrated intensity of the 5.9- or 5.1-nm actin layer lines. Together with the assumption that in rigor 100% of the myosin heads are bound to actin whereas under relaxing conditions no cross-bridges contribute to the intensity of 5.9- and 5.1-nm actin layer lines (Xu et al., 1997; Kraft et al., 1999), the square root of the observed changes in integrated intensities provides an estimate of the number of strongly attached cross-bridges. The fractions of strongly attached cross-bridges shown in Table 1 (middle column) were derived from the experimentally observed increase in intensity during isometric contraction over the intensity during relaxation ($\Delta I_{\text{Isometric}}$) and related to the change in rigor ($\Delta I_{\text{Isometric}}/\Delta I_{\text{rigor}}$; Table 1, left column).

However, in an attempt to test the validity of this estimate and to account for structural differences between strongly attached cross-bridges in rigor and during isometric contraction, model calculations were carried out based on the F-actin structure decorated by S1. The coordinate files were from Lorenz et al. (1993), and groups of eight consecutive amino acid residues were combined to spheres of equivalent mass. To account for the mismatch between actin and myosin periodicities, the S1-molecules were bent in axial and azimuthal direction. Bending of up to ±25 Å was allowed, which was assigned to the regulatory light-chain (LC) binding region of the S1 molecule (Rayment et al., 1993) or, alternatively, the entire LC binding region plus approximately one-third of the motor domain was rotated about a hinge at the SH1-SH2-helix. The occupancy of actin monomers by stereospecifically attached cross-bridges was varied from 16% to 74%. Intensity profiles of the actin layer lines in the calculated patterns were determined. These intensity profiles, particularly the ones obtained from the actomyosin models, which are presumably closest to the underlying structure, were rather similar to the experimentally obtained intensity profiles (details will be published elsewhere). The intensity increase of the 5.9- and 5.1-nm actin layer line was plotted as a function of the fraction of attached myosin heads (Fig. 6). The relations between increase in integrated intensity versus fraction of attached myosin heads were not much affected by the nature of the distortion of the myosin heads and were rather close to the relation expected from the square law. The experimentally observed intensity changes (Table 1, left column) were compared with the

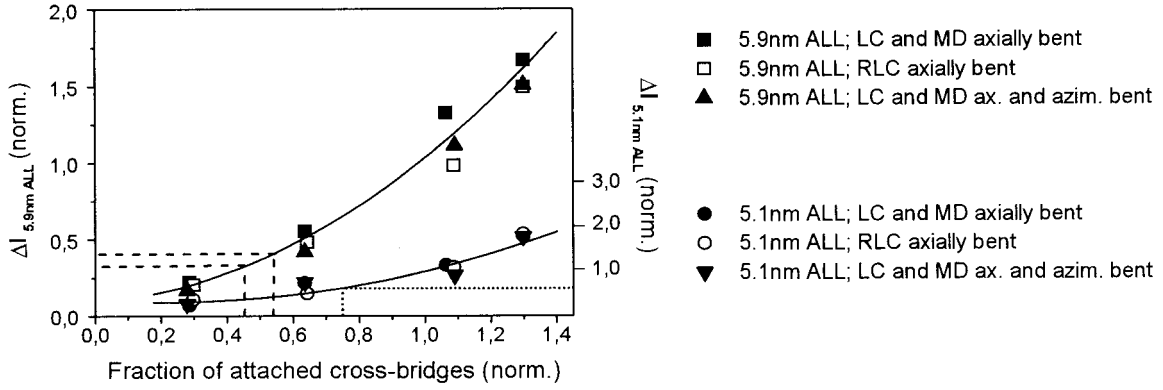

FIGURE 6 Relation between increase in integrated intensities of actin layer lines and fraction of S1 attached to F-actin calculated from a model of actin with attached S1 molecules with different types of distortion. Either the light chain binding region (LC) plus approximately one-third of the motor domain (MD) or, alternatively, only the regulatory light-chain binding region (RLC) of the S1 molecule was axially bent by up to ±25 Å. As a third alternative, the LC-binding region plus approximately one-third of the MD were axially and azimuthally bent by up to ±25 Å. For all three types of distortion the increase in integrated intensities of the 5.9-nm and the 5.1-nm actin layer line (ALL) are shown. The lines through the data points are polynomial fits to the average of the values for the 5.9 and the 5.1-nm ALL, respectively. The fraction of attached cross-bridges of 1.0 corresponds to 57% of the actin monomers occupied by myosin heads, which is the maximal occupancy possible in muscle fibers in rigor. The model calculations were carried out for up to 74% of actin monomers occupied by myosin heads. The intensity changes of the 5.9- and the 5.1-nm ALL found for 57% of actin monomers occupied by myosin heads (fraction 1.0) are also set to 1.0. The dashed and dotted lines indicate how from the experimentally obtained intensity changes shown in Table 1 (left column) the fractions of attached myosin heads (Table 1, right column) were obtained (e.g., if $\Delta I_{59} = 0.33$, then n (from modeling) = 0.45). Note that even for different bending modes our data cannot account for very low fractions of attached cross-bridges during isometric force generation.

intensity increases of the actin layer lines found by modeling for attachment of different fractions of cross-bridges as shown in Fig. 6 (dashed and dotted lines), and the resulting fractions are shown in Table 1, right column. In Fig. 6 the fraction attached of 1.0 corresponds to 57% of the actin monomers occupied by myosin heads, which is the highest possible occupancy in rigor muscle fibers due to the ratio of myosin heads to actin monomers. Therefore, the intensity increase (ΔI) of the 5.9- and the 5.1-nm actin layer lines found for attachment of myosin heads to 57% of actin monomers was also set to 1.0. From the data in Table 1, it can be concluded that the experimentally seen intensification of the unsampled actin layer lines in isometric contraction can be modeled by stereospecific (and strong) attachment between 50% (for the 5.9-nm actin layer line) and 75% (for the 5.1-nm actin layer line) of all myosin heads to actin. The difference between the two layer lines presumably at least in part is due to effects of the specific myosin head structure on the intensity of the 5.9- and the 5.1-nm actin layer line (see Fig. 6) but additional, more detailed modeling is required to solve this question. Nevertheless, even the lower limit of 50% of the myosin heads stereospecifically attached to actin during isometric contraction is still a much higher estimate than recently suggested by others (e.g., Huxley and Kress, 1985; Irving et al., 1995; Holmes, 1997).

In the past there have been other explanations for the intensity increase of the actin layer lines during contraction. Based on their own data, Wakabayashi and coworkers postulated that the intensity increase of the actin layer lines in contraction is solely due to a structural change within the thin filament (Wakabayashi et al., 1991). This structural change was assumed to be induced by interaction of myosin heads with actin and to affect the whole actin filament in a cooperative way. In modeling studies these authors showed that their experimentally observed changes in actin layer line intensities could be modeled by a change in the domain structure of the actin monomer together with a change of the tropomyosin position on the thin filament. This conclusion, however, is based on data that show no increase in the first actin layer line intensity during isometric contraction and no shift in intensity distribution of the 5.9-nm actin layer line toward the meridian when compared with relaxing conditions. In similar model calculations it was shown that actin subdomain movement plus a tropomyosin shift can explain the intensity changes of the actin layer lines upon calcium activation at a sarcomere length beyond overlap (Al-Khayat et al., 1995; Harford and Squire, 1997), i.e., an intensity decrease on the first and an increase on the 5.9- and 5.1-nm actin layer lines without a shift in intensity distribution. But such a reciprocal change of the intensity on the first actin layer line versus the 5.9- and 5.1-nm actin layer lines is not consistent with the experimental data shown in our work and the work of others. Thus, modeling of subdomain movement plus a shift in the position of tropomyosin but without attachment of myosin heads so far was not able to account for the intensity changes in contraction at full overlap, namely the increase in the first, the 5.9-, and the 5.1-nm actin layer line intensities, as well as the shift of the intensity maximum on the 5.9-nm actin layer line toward the meridian.

Studying the effect of calcium on the 5.9-nm actin layer line in the presence of the nonhydrolyzable nucleotide analog MgATPγS also showed an intensity increase at long sarcomere length and a slightly larger increase at normal sarcomere length but no shift in intensity distribution (Kraft et al., 1999). This indicates that at least weakly bound cross-bridges, like cross-bridges with MgATPγS, at high calcium concentration cannot induce structural changes within the actin filament that would result in a substantial intensity increase and a shift in the intensity maximum as observed in isometric contraction. Maeda and coworkers, who also observed an increase and a shift of the 5.9-nm actin layer line, at least at 1°C and 10°C in frog muscle, showed that this increase is linearly dependent on thin and thick filament overlap (Maeda et al., 1988). This strongly supports the idea that this increase is at least partly due to cross-bridge binding. However, until appropriate model calculations are available, which also include effects of the troponin complex, we cannot rule out that (part of) the observed intensity changes of the actin layer lines during active contraction arise from structural changes within the actin filament, possibly induced by cross-bridge binding.

Nevertheless, the data presented here are consistent with the idea that during isometric contraction a large fraction of cross-bridges is stereospecifically (strongly) attached to actin in a nonrigor-like conformation. The results indicate that it is rather unlikely that cross-bridges during force generation have a structure similar to the nucleotide-free actomyosin complex. Previously it was proposed that isometric force is generated already at the transition from a weakly bound (nonstereospecific) to a stereospecifically and strongly bound state (Brenner, 1991; Brenner et al., 1995). Based on this concept, our data seem to imply that the intensification of the actin layer line is due to a large fraction of cross-bridges, which contributes to force generation, instead of being in a strongly bound but preforce generating state.

The authors would like to thank S. Xu, D. Gilroy, G. Melvin, and L. C. Yu (National Institutes of Health, NIAMS, Bethesda, MD), S. Slawson (SRS Daresbury, United Kingdom), G. Rapp (EMBL-outstation, DESY, Hamburg, Germany), as well as T. Scholz, B. Heins-Höntsch, and M. Hoppe (Medical School Hannover, Germany) for their contribution to this work. The work was supported by the EU "Access to large facilities"-program and by the Deutsche Forschungsgemeinschaft (Br849/12-1).

REFERENCES

Al-Khayat, H. A., N. Yagi, and J. M. Squire. 1995. Structural changes in actin-tropomyosin during muscle regulation: computer modelling of low-angle X-ray diffraction data. *J. Mol. Biol.* 252:611–632.

Bershitsky, S. Y., A. K. Tsaturyan, O. N. Bershitskaya, G. I. Mashanov, P. Brown, R. Burns, and M. A. Ferenczi. 1997. Muscle force is generated by myosin heads stereospecifically attached to actin. *Nature.* 388: 186–190.

Brenner, B. 1983. Technique for stabilizing the striation pattern in maximally calcium-activated skinned rabbit psoas fibers. *Biophys. J.* 41: 99–102.

Brenner, B. 1991. Rapid dissociation and reassociation of actomyosin cross-bridges during force generation: a newly observed facet of cross-bridge action in muscle. *Proc. Natl. Acad. Sci. U. S. A.* 88:10490–10494.

Brenner, B., J. M. Chalovich, and L. C. Yu. 1995. Distinct molecular processes associated with isometric force generation and rapid tension recovery after quick release. *Biophys. J.* 68:106S–111S.

Brenner, B., S. Xu, J. M. Chalovich, and L. C. Yu. 1996. Radial equilibrium lengths of actomyosin cross-bridges in muscle. *Biophys. J.* 71: 2751–2758.

Brenner, B., and L. C. Yu. 1993. Structural changes in the actomyosin cross-bridges associated with force generation. *Proc. Natl. Acad. Sci. U. S. A.* 90:5252–5256.

Brenner, B., L. C. Yu, and R. J. Podolsky. 1984. X-ray diffraction evidence for cross-bridge formation in relaxed muscle fibers at various ionic strengths. *Biophys. J.* 46:299–306.

Cooke, R., M. S. Crowder, and D. D. Thomas. 1982. Orientation of spin labels attached to cross-bridges in contracting muscle fibres. *Nature.* 300:776–778.

Cooke, R., M. S. Crowder, C. H. Wendt, V. A. Barnett, and D. D. Thomas. 1984. Muscle cross-bridges: do they rotate? *Adv. Exp. Med. Biol.* 170: 413–427.

Cooke, R., and K. Franks. 1980. All myosin heads form bonds with actin in rigor rabbit skeletal muscle. *Biochemistry.* 19:2265–2269.

Fajer, P. G., E. A. Fajer, and D. D. Thomas. 1990. Myosin heads have a broad orientational distribution during isometric muscle contraction: time-resolved EPR studies using caged ATP. *Proc. Natl. Acad. Sci. U. S. A.* 87:5538–5542.

Furch, M., M. A. Geeves, and D. J. Manstein. 1998. Modulation of actin affinity and actomyosin adenosine triphosphatase by charge changes in the myosin motor domain. *Biochemistry.* 37:6317–6326.

Geeves, M. H., and K. C. Holmes. 1999. Structural mechanism of muscle contraction. *Annu. Rev. Biochem.* 68:687–728.

Harford, J., and J. Squire. 1997. Time-resolved studies of muscle using synchrotron radiation (review). *Rep. Prog. Phys.* 60:1723–1787.

Haselgrove, J. C. 1975. X-ray evidence for conformational changes in the myosin filaments of vertebrate striated muscle. *J. Mol. Biol.* 92:113–143.

Hill, T. L. 1974. Theoretical formalism for the sliding filament model of contraction of striated muscle: part I. *Prog. Biophys. Mol. Biol.* 28: 267–340.

Hirose, K., T. D. Lenart, J. M. Murray, C. Franzini-Armstrong, and Y. E. Goldman. 1993. Flash and smash: rapid freezing of muscle fibers activated by photolysis of caged ATP. *Biophys. J.* 65:397–408.

Holmes, K. C. 1997. The swinging lever-arm hypothesis of muscle contraction. *Curr. Biol.* 7:R112–R118.

Huxley, H. E., and W. Brown. 1967. The low-angle x-ray diagram of vertebrate striated muscle and its behaviour during contraction and rigor. *J. Mol. Biol.* 30:383–434.

Huxley, H. E., A. R. Faruqi, M. Kress, J. Bordas, and M. H. Koch. 1982. Time-resolved X-ray diffraction studies of the myosin layer-line reflections during muscle contraction. *J. Mol. Biol.* 158:637–684.

Huxley, H. E., and M. Kress. 1985. Crossbridge behaviour during muscle contraction. *J. Muscle Res. Cell Motil.* 6:153–161.

Irving, M., T. St. Claire Allen, C. Sabido-David, J. S. Craik, B. Brandmeier, J. Kendrick-Jones, J. E. Corrie, D. R. Trentham, and Y. E. Goldman. 1995. Tilting of the light-chain region of myosin during step length changes and active force generation in skeletal muscle [see comments]. *Nature.* 375:688–691.

Kraft, T., and B. Brenner. 1997a. Cross-bridge conformation during isometric contraction and in the presence of nucleotide analogs: a 2D-X-ray diffraction study on single muscle fibers. *Biophys. J.* 72:A1.

Kraft, T., and B. Brenner. 1997b. Force enhancement without changes in cross-bridge turnover kinetics: the effect of EMD 57033. *Biophys. J.* 72:272–281.

Kraft, T., J. M. Chalovich, L. C. Yu, and B. Brenner. 1995. Parallel inhibition of active force and relaxed fiber stiffness by caldesmon

fragments at physiological ionic strength and temperature conditions: additional evidence that weak cross-bridge binding to actin is an essential intermediate for force generation. *Biophys. J.* 68:2404–2418.

Kraft, T., T. Mattei, and B. Brenner. 1998. Structural features of force-generating cross-bridges: a 2D-X-ray diffraction study. *Adv. Exp. Med. Biol.* 453:289–295.

Kraft, T., T. Mattei, A. Radocaj, and B. Brenner. 2000. Actin layer line profiles of single skinned fibers of rabbit psoas muscle during isometric contraction, relaxation and rigor at 20°C. *Biophys. J.* 78:228A.

Kraft, T., S. Xu, B. Brenner, and L. C. Yu. 1999. The effect of thin filament activation on the attachment of weak binding cross-bridges: a two-dimensional x-ray diffraction study on single muscle fibers. *Biophys. J.* 76:1494–1513.

Kraft, T., L. C. Yu, H. J. Kuhn, and B. Brenner. 1992. Effect of Ca2+ on weak cross-bridge interaction with actin in the presence of adenosine 5′-[gamma-thio]triphosphate). *Proc. Natl. Acad. Sci. U. S. A.* 89: 11362–11366.

Kress, M., H. E. Huxley, A. R. Faruqi, and J. Hendrix. 1986. Structural changes during activation of frog muscle studied by time-resolved x-ray diffraction. *J. Mol. Biol.* 188:325–342.

Lorenz, M., D. Popp, and K. C. Holmes. 1993. Refinement of the F-actin model against X-ray fiber diffraction data by the use of a directed mutation algorithm. *J. Mol. Biol.* 234:826–836.

Lovell, S. J., and W. F. Harrington. 1981. Measurement of the fraction of myosin heads bound to actin in rabbit skeletal myofibrils in rigor. *J. Mol. Biol.* 149:659–674.

Lowy, J., and F. R. Poulsen. 1987. X-ray study of myosin heads in contracting frog skeletal muscle. *J. Mol. Biol.* 194:595–600.

Maeda, Y., D. Popp, and S. M. McLaughlin. 1988. Cause of changes in the thin filament-associated reflexions on activation of frog muscle–myosin binding or conformational change of actin. *Adv. Exp. Med. Biol.* 226: 381–390.

Parry, D. A., and J. M. Squire. 1973. Structural role of tropomyosin in muscle regulation: analysis of the x-ray diffraction patterns from relaxed and contracting muscles. *J. Mol. Biol.* 75:33–55.

Poulsen, F. R., and J. Lowy. 1983. Small-angle X-ray scattering from myosin heads in relaxed and rigor frog skeletal muscles. *Nature.* 303: 146–152.

Rapp, G., K. Guth, Y. Maeda, K. J. Poole, and R. S. Goody. 1991. Time-resolved X-ray diffraction studies on stretch-activated insect flight muscle. *J. Muscle Res. Cell Motil.* 12:208–215.

Rayment, I., W. R. Rypniewski, K. Schmidt-Base, R. Smith, D. R. Tomchick, M. M. Benning, D. A. Winkelmann, G. Wesenberg, and H. M. Holden. 1993. Three-dimensional structure of myosin subfragment-1: a molecular motor. *Science.* 261:50–58.

Roopnarine, O., and D. D. Thomas. 1995. Orientational dynamics of indane dione spin-labeled myosin heads in relaxed and contracting skeletal muscle fibers. *Biophys. J.* 68:1461–1471.

Squire, J. M. 1981. The Structural Basis of Muscular Contraction. Plenum Press, New York, London.

Tsaturyan, A. K., S. Y. Bershitsky, R. Burns, and M. A. Ferenczi. 1999. Structural changes in the actin-myosin cross-bridges associated with force generation induced by temperature jump in permeabilized frog muscle fibers. *Biophys. J.* 77:354–372.

Wakabayashi, K., H. Tanaka, Y. Amemiya, A. Fujishima, T. Kobayashi, T. Hamanaka, H. Sugi, and T. Mitsui. 1985. Time-resolved x-ray diffraction studies on the intensity changes of the 5.9 and 5.1 nm actin layer lines from frog skeletal muscle during an isometric tetanus using synchrotron radiation. *Biophys. J.* 47:847–850.

Wakabayashi, K., H. Tanaka, H. Saito, N. Moriwaki, Y. Ueno, and Y. Amemiya. 1991. Dynamic X-ray diffraction of skeletal muscle contraction: structural change of actin filaments. *Adv. Biophys.* 27:3–13.

Williams, D. L., Jr., L. E. Greene, and E. Eisenberg. 1984. Comparison of effects of smooth and skeletal muscle tropomyosins on interactions of actin and myosin subfragment 1. *Biochemistry.* 23:4150–4155.

Xu, S. G., M. Kress, and H. E. Huxley. 1987. X-ray diffraction studies of the structural state of crossbridges in skinned frog sartorius muscle at low ionic strength. *J. Muscle Res. Cell Motil.* 8:39–54.

Xu, S., S. Malinchik, D. Gilroy, T. Kraft, B. Brenner, and L. C. Yu. 1997. X-ray diffraction studies of cross-bridges weakly bound to actin in relaxed skinned fibers of rabbit psoas muscle. *Biophys. J.* 73:2292–2303.

Yagi, N., and I. Matsubara. 1988. Changes in the 5.9 nm actin layer-line on activation of frog skeletal muscles. *Adv. Exp. Med. Biol.* 226:369–380.

Yu, L. C., and B. Brenner. 1989. Structures of actomyosin crossbridges in relaxed and rigor muscle fibers. *Biophys. J.* 55:441–453.